Eur. Phys. J. D **8**, 265–272 (2000)

THE EUROPEAN PHYSICAL JOURNAL D

EDP Sciences

Evidence for $N^{1/3}$ dependence of the sticking cross-section of atoms on small and medium-size van der Waals clusters

J. Vigué, P. Labastie, and F. Calvo[a]

Laboratoire Collisions, Agrégats, Réactivité[b], IRSAMC, Université Paul Sabatier, 118 route de Narbonne, 31062 Toulouse Cedex 4, France

Received 20 May 1999 and Revised in final form 22 July 1999

Abstract. This paper introduces a simple model describing the cluster growth in supersonic expansions. The predicted terminal mean cluster size is compared to the available data in the case of argon. The agreement between the model and the experimental results requires that the cross-section describing the sticking of an atom on a cluster of size N scales like N^α with α in the range 0.34–0.44, well below the $\alpha = 2/3$ predicted by the simplest geometrical scaling argument. We explain this unexpected result in two steps. First, using Monte Carlo simulations, we check that the potential between an atom and a cluster is accurately represented by the Gspann and Vollmar potential, even at finite temperature. Then, using Langevin's approximation, we show that the sticking cross-section scales like $N^{1/3}$ for small to moderate N values and switches to the geometric scaling $N^{2/3}$ for very large N values. The crossover between these two scalings occurs when $N \approx 10^3$ for argon, but the mean exponent α over the size range 1–10^4 is 0.46. This N scaling of the sticking cross-section should play an important role whenever condensation is important as it modifies the kinetics of the early stages.

PACS. 34.50.-s Scattering of atoms, molecules, and ions – 36.40.-c Atomic and molecular clusters – 64.60.Qb Nucleation

1 Introduction

Supersonic expansions are very commonly used to produce clusters of atoms and molecules. The number N of monomers in a cluster can be easily varied by changing the parameters of the source (its temperature, its pressure, the nozzle diameter and shape). A very wide range of sizes N can thus be covered from a few unities up to almost any value. Several works [1–7] have been devoted to the measurement of the mean size $\langle N \rangle$ with the source parameters, the results covering the range 1–10^4 in the case of argon. Many results are available in the particular case of permanent gases, mostly rare gases, because the source pressure can then be easily varied in a very wide range. The striking point is the very rapid variation of the mean size $\langle N \rangle$ with the source pressure p_0. Several empirical scaling laws [5] have been proposed to relate the cluster mean size $\langle N \rangle$ to a scaling parameter Γ^* introduced by Hagena, see reference [8] and references cited therein. In the case of argon, this scaling parameter is given by [5]:

$$\Gamma^* = 1646 p_0 d_{\rm eq}^{0.85} / T_0^{2.2875}, \qquad (1)$$

where the source pressure p_0 is expressed in mbar, the equivalent diameter $d_{\rm eq}$ of the nozzle in micrometer and the source temperature T_0 in kelvin. Expressions analogous to equation (1) for most gases of interest have been given by Hagena and coworkers [9].

In Section 2, we have developed a simple model for cluster growth in such an expansion. This model gives a relation between the cluster size and the source conditions, and this relation depends on the relation between the sticking cross-section and the cluster size. The surprising feature is that the model reproduces the observations only if this cross-section is proportional to N^α with $\alpha \approx 1/3$ and not with $\alpha = 2/3$ as the usual dimensional argument would predict: the scale length in a cluster of size N increases like $N^{1/3}$ and a cross-section, being of the dimension of an area, should behave like $N^{2/3}$.

This experimental evidence may not be fully convincing as it assumes the validity of our simple model. We have therefore demonstrated this property. In a first step (Sect. 3), we calculate the atom-cluster potential at finite temperature using the potential of Gspann and Vollmar [10,11] and numerical simulations. Then, in Section 4, using this potential function and a Langevin-type calculation, we have estimated the capture cross-section of an atom by a cluster of size N. The calculated cross-section increases with cluster size as $N^{1/3}$ at relatively low N values when the dominant effect is due to the long-range

[a] *Present address*: Département de Recherche Fondamentale sur la Matière Condensée, SI2A, CEA Grenoble, 17 rue des Martyrs, 38054 Grenoble Cedex 9, France.
e-mail: `fcalvo@cea.fr`

[b] UMR 5589 du CNRS

$1/r^6$ potential. As expected, a $N^{2/3}$ behaviour is finally observed for sufficiently large N values. In the case of argon, the crossover between these two regimes occurs near $N \approx 1000$, and this is in agreement with the interpretation of the experimental results done with our model.

2 Simple model for cluster growth in free jets

2.1 Model

To describe the growth of a cluster during a supersonic expansion, the simplest model one can think of is the following. In a first step, very small clusters are formed by 3-body collisions: this step will not be discussed as it does not limit the final size. In a second step, some of these very small clusters grow by addition of individual atoms following the reactions:

$$A_N + A \longrightarrow A^*_{N+1} \tag{2}$$

where the $*$ indicates a cluster with a large internal energy. These clusters are stabilized by evaporation of a hot atom:

$$A^*_{N+1} \longrightarrow A_N + A. \tag{3}$$

In this matter, our model differs from other models for cluster growth [1,8,9,12] because we do not consider the possibility that a bimolecular gas-cluster collision can stabilize the cluster, and we treat unimolecular evaporation as the only stabilization process. This seems a realistic idea if one considers the evaporative ensemble theory of Klots [13] as well as dynamical simulations [14].

Provided that there are on average more addition than evaporation processes, the clusters grow. This kinetic scheme can be described by the following equation relating the average cluster size N to the local monomer density n_1:

$$\frac{\mathrm{d}N}{\mathrm{d}t} = n_1(t)\sigma_N v_\mathrm{r}. \tag{4}$$

Here σ_N is the effective cross-section describing the sticking collision of an atom on a cluster of size N, resulting from the total effect of capture and evaporation processes. Equation (4) means that we assume the limiting step in the kinetics of cluster growth to be bimolecular collisions which add atoms to the cluster, so that the kinetic behaviour is dominated by bimolecular processes only. This point will be further discussed in Section 4.2.

This effective cross-section should be a fraction of the capture cross-section which scales with N like N^α, as shown below. Therefore we can write:

$$\sigma_N = \sigma_1 N^\alpha. \tag{5}$$

The equation describing the variations of N is easy to integrate if we make a series of simplifying assumptions. First of all, we assume that the monomer density $n_1(t)$ is the free jet value, with negligible depletion. Using the results of references [15,16], when the distance z from the nozzle is considerably larger than the nozzle diameter d_0, ($z \gg d_0$), the density $n_1(z)$ is given by

$$n_1(z) = n_0 f(z^*), \tag{6}$$

where $z^* = z/d_0$ and with the function $f(z^*)$ given by

$$f(z^*) = z^{*-2}\left[\frac{2}{(\gamma-1)A^2}\right]^{1/(\gamma-1)}, \tag{7}$$

γ being the specific heat ratio. A is a parameter deduced from flow simulations. From now on, we consider only the case of a monoatomic gas with $\gamma = 5/3$. The value of A in this case is available: $A = 3.26$ following [15] and $A = 3.337$ following [16]. Using this last value of A, equation (7) becomes $f(z^*) = 0.14 z^{*-2}$. The hydrodynamic flow velocity rapidly reaches its asymptotic value u given by

$$u = \left[\frac{2\gamma k_\mathrm{B} T_0}{(\gamma-1)m}\right]^{1/2} = \left[\frac{5k_\mathrm{B}T_0}{m}\right]^{1/2}, \tag{8}$$

so that we can make the usual assumption that the distance z from the nozzle and the time t are linearly related, $z = ut$. The local temperature is given by an equation similar to the one giving the density:

$$\begin{aligned} T(z) &= \left[\frac{2}{(\gamma-1)A^2}\right] z^{*-2(\gamma-1)} T_0 \\ &= 0.27 z^{*-4/3} T_0 \end{aligned} \tag{9}$$

in the present case of a monoatomic gas. The application of equations (7–9) to polyatomic gases is possible only if the ratio of specific heats is constant, an assumption which is usually not correct. The equation giving $T(z)$ ceases to be valid as soon as condensation starts. In the region where the clusters are formed, the local density $n_1(z)$ and the local temperature $T(z)$ must follow the border of the condensation domain (this should be very close to the usual liquid-gas or solid-gas coexistence curve, slightly corrected by the finite size of the clusters). As this curve is almost vertical in the density-temperature plane, the internal temperature of the beam should be almost constant and we note T_c its value. Obviously this is a rough approximation, and one should not forget that the beam is not in thermal equilibrium, the gas being colder than the cluster. The equation $T(z) = T_\mathrm{c}$ will be used to determine at which position z_c condensation starts (we note $z^*_\mathrm{c} = z_\mathrm{c}/d_0$). We can assume that the relative atom-cluster velocity v_r has a constant value given by the usual formula (it is a good approximation to replace the atom-cluster reduced mass by the atomic mass m as soon as the cluster size N is not too small):

$$v_\mathrm{r} = \sqrt{\frac{8k_\mathrm{B}T_\mathrm{c}}{\pi m}}\,. \tag{10}$$

Changing to the z^* variable, the equation giving N can be written as

$$\frac{\mathrm{d}N}{\mathrm{d}z^*} = 0.14 n_0 \sigma_1 d_0 \frac{v_\mathrm{r}}{u z^{*2}} N^\alpha. \tag{11}$$

The integration of this equation is straightforward. It should be made only for z^* values greater than z_c^*. The final value N_f of N is given by:

$$N_f = \left[\frac{0.14 n_0 \sigma_1 d_0 v_r}{(1-\alpha) u z_c^*}\right]^{1/(1-\alpha)} = \Gamma_{th}^{1/(1-\alpha)}. \quad (12)$$

We have introduced a "theoretical" Γ parameter Γ_{th} defined by

$$\Gamma_{th} = 0.14 n_0 \sigma_1 d_0 v_r / \left[(1-\alpha) u z_c^*\right]. \quad (13)$$

We will show in Section 4 that, within a constant multiplying factor, this parameter is very close to the scaling parameter Γ^* introduced by Hagena [8,12] from an analysis of the kinetics of free jets expansions.

The experimental results described in references [4–6] can be represented by scaling laws of the type:

$$N_f \approx \Gamma^{*\beta}. \quad (14)$$

The data collected by Lallement [4] covers a range of source pressure from 2 to 30 bars and of N values from 50 to 4000. From this plot, we have deduced a β value equal to $\beta = 1.51$. The data collected by Benslimane [6] extends this range to 30 bars and $N = 7000$ and we have found that it is very well represented by a slightly larger value $\beta = 1.64$. The published values [5] (and references therein) of β are $\beta = 1.64$ for low Γ^* values ($350 < \Gamma^* < 1800$) and $\beta = 2.35$ for larger Γ^* values ($\Gamma^* > 1800$). This last scaling law is not in very good agreement with the data. An other scaling law fits better the experimental data: $N = \exp\left[-12.83 + 3.51(\ln \Gamma^*)^{0.8}\right]$, and it is easy to verify that, for this law, the logarithmic slope β decreases from 1.88 to 1.80 when Γ^* varies from 1800 to 10^4.

We can deduce an estimated value of α from these experimental results: $\alpha = 1 - \beta^{-1}$. We thus obtain values in the range $\alpha = 0.34$–0.44 when β covers the range 1.51–1.80. These α values are slightly larger than 1/3 and considerably lower than the values 2/3 predicted by the simple geometric scaling law described above.

2.2 Discussion and refinements of the model

A severe assumption of the model described above is that it assumes no depletion of the monomer density by formation of the clusters. This assumption is not verified experimentally. The experiments are also able to measure the residual content of monomers in the beam and the results of such measurements are that the residual monomer content is negligible when the source pressure is large. Typically, for pure argon near ordinary temperature, with a nozzle diameter equal to 0.1 mm, this occurs for $p_0 > 7$ bar [4,17]. This means that we should refine our model to take this depletion into account. We introduce the cluster density $n_{cl}(z)$ and we write the conservation of the total atomic density as:

$$n_1(z) + n_{cl}(z) N(z) = n_0 f(z^*) \quad (15)$$

which can be re-expressed, using the fraction of monomers $x_1(z) = n_1(z)/n_0 f(z^*)$ and the fraction of clusters $x_{cl}(z) = n_{cl}(z)/n_0 f(z^*)$, as

$$x_1(z) + x_{cl}(z) N(z) = 1. \quad (16)$$

The depletion of monomers due to the cluster growth leads to:

$$\frac{dx_1}{dz} = -x_{cl} \frac{dN}{dz}. \quad (17)$$

To write this equation, we have made the assumption that we could neglect the variation of the number of clusters along the flow. This is surely wrong in the beginning of the expansion, but this seems a reasonable assumption in the following stages. With the equation giving the variation of N with z, we have now a set of three nonlinear equations. After elimination of x_{cl}, we get:

$$\frac{dN}{dz^*} = x_1 N^\alpha \Gamma_{th} z_c^* f(z^*); \quad (18)$$

$$\frac{dx_1}{dz^*} = -x_1(1-x_1) N^{\alpha-1} \Gamma_{th} z_c^* f(z^*). \quad (19)$$

This system of nonlinear equations has an interesting property. For any value of $\alpha \neq 0$, we can introduce a reduced value N^* of the cluster size N defined by $N^* = N \Gamma_{th}^{1/(1-\alpha)}$. With this change of variable, the system takes a form independent of the parameter Γ_{th}:

$$\frac{dN^*}{dz^*} = x_1 N^{*\alpha} z_c^* f(z^*); \quad (20)$$

$$\frac{dx_1}{dz^*} = -x_1(1-x_1) N^{*(\alpha-1)} z_c^* f(z^*). \quad (21)$$

The fact that this system is independent of the parameter Γ_{th} proves immediately that the final value of N is proportional to $\Gamma_{th}^{1/(1-\alpha)}$. Therefore the measurement of the slope of the cluster size N as a function of Γ_{th} should give access to α even when the monomer content of the beam is very small at the end of the expansion.

3 Cluster-atom interaction at finite temperature

In order to calculate the sticking cross-section of an atom on a cluster of size N, we first need to estimate the potential undergone by the atom approaching the cluster. Indeed, what we especially need is its variations with the distance r, as well as with the size N itself. At zero temperature, one can model the interaction between any two argon atoms by the commonly used Lennard-Jones (LJ) 12–6 potential. A simple model for the cluster is to represent it by a sphere of homogeneously distributed LJ centres. This model, first proposed by Gspann and Vollmar [10,11], leads to the following expression for the interaction between an Ar_N cluster and an Ar atom separated

by distance r to the cluster centre of mass:

$$V_N(r) = C_{12}\frac{r^6 + 21r^4r_0^2/5 + 3r^2r_0^4 + r_0^6/3}{(r^2 - r_0^2)^9} - \frac{C_6}{(r^2 - r_0^2)^3}\,. \quad (22)$$

The parameters C_{12}, C_6 and r_0 are size-dependent and their values are given by $C_6(N) = 4N\varepsilon\sigma^6$, $C_{12} = 4N\varepsilon\sigma^{12}$ and $r_0(N) = (3/4\pi\rho)^{1/3}[N^{1/3} - 1] = r^*[N^{1/3} - 1]$ where ε and σ are the LJ parameters for the atom-atom potential: $V_1(r) = 4\varepsilon[(\sigma/r)^{12} - (\sigma/r)^6]$. ρ is the atomic density in the solid state, and $r^* = 2.08$ Å for argon [5], which corresponds to 0.62 reduced units σ. As N goes to ∞, this potential also recovers the correct form of the interaction between an atom and a surface [18]. Gspann and Vollmar (GV) introduced this potential to calculate atom or molecules-clusters scattering and sticking cross-sections [10,11]. The GV potential has been used by Buck and Krohne for the experimental determination of the size of argon clusters probed by scattering of a helium molecular beam [5].

Rigorously, this model can only be valid at zero temperature, as the cluster cannot reorganize by itself to permit merging of the approaching atom below $r \leq r_0$. In reality, even for high pressures, temperatures are nonzero inside the expansion, and the atoms inside the cluster can move, especially when the cluster is in a "liquidlike" thermodynamical phase.

Another problem is that clusters are non spherical, at least up to a reasonable size of several hundred argon atoms. Instead, they may frequently have icosahedral shapes, or some elements with pentagonal symmetry. When such a case occurs (*e.g.* with the perfect multilayer Mackay icosahedra $N = 13$, 55, 147...), the interaction with an external atom strongly varies with the cluster orientation, and the observed potential is different depending on whether the atom is closer to a vertex, an edge or a face [5]. This concerns specially the repulsive contribution of the potential (C_{12} term) which is important at short distances.

To circumvent this problem, a possible idea would be to perform averages on the cluster orientation. However, as the influence of the extra atom gets stronger as the atom gets closer, it could be necessary to give unequal weights to different orientations, so that these weights should be functions of the distance r. Such an approach seems quite non trivial.

A much more straightforward way to test the validity of the GV potential of equation (22) in the "real case" of finite-temperature clusters is the direct numerical simulation. In a first step, we still need to investigate the zero temperature case to serve as a reference for the further free-energy calculations. At zero temperature, the absolute interaction energy at fixed distance r from the atom to the cluster center of mass can be calculated with the usual global optimization methods [19]. Constraining forces must then be added to keep the distance r to a prescribed value. When r is large enough, the cluster structure is not modified by the extra atom, only its orientation can rearrange. As r decreases, isomerization processes (reorientations) may occur to further stabilize the Ar_N+Ar configuration. Finally, when r gets below the typical cluster radius, the $N + 1$ atoms cannot be distinguished and the optimization becomes meaningless.

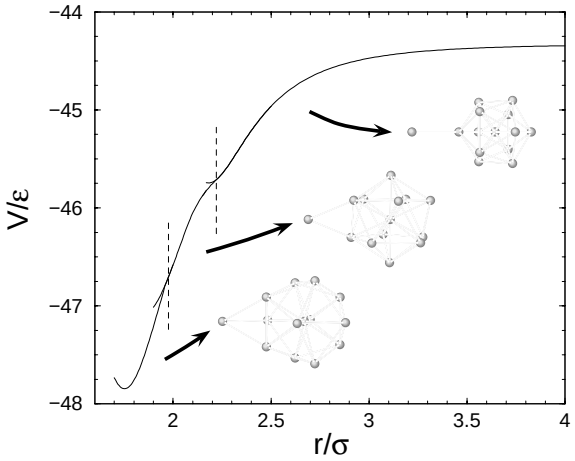

Fig. 1. Minimum-energy path for the Ar_{13}+Ar system at long-distance and zero temperature. The three configurations shown are stable at fixed distance between the cluster centre of mass and the extra atom.

Such spontaneous isomerization are seen, for instance, in the case of the icosahedral Ar_{13} cluster. At long distance, the fourteenth external atom is on a C_5 axis in order to be closer to a surface atom. Below $r \sim 2.2\sigma$ (about 7.5 Å with the standard value 3.4 Å for σ), the icosahedron tends to rotate, permitting the colliding atom to lie over an edge. At last, below $r \sim 1.95\sigma$ (about 6.7 Å), it rotates again to have the 14th atom located on the center of a triangular facet. The corresponding interaction energy is plotted in Figure 1 along with the three described configurations. Obviously, as the cluster size increases, the number of possible isomerizations also rapidly increases. These phenomena are characteristic of "real" clusters made of a finite number of atoms, and any comparison to the previous continuous model should be limited to values of r ensuring only a single isomer at zero temperature.

The calculation of effective interaction energies at finite temperature relies on specific methods. The potential of mean force (PMF) is the free-energy difference ΔA between a configuration at distance r and a reference configuration at distance r^* which may be ∞. The simplest way to compute the PMF is the thermodynamic integration technique. This method [19] provides the derivative $\partial A/\partial r$ along the reaction coordinate $\{r\}$ with the following equation:

$$\frac{\partial A}{\partial r}(r,T) = \left\langle \frac{\partial V}{\partial r} \right\rangle_{r,T} \quad (23)$$

where V is the potential-energy function, T the temperature and $\langle\cdot\rangle_{r,T}$ the canonical average at fixed r and T. Knowing the derivatives of A, the PMF can be numerically estimated up to an additive constant over the entire path of $\{r\}$. A more complete description of this method (and others such as umbrella sampling) applied to similar

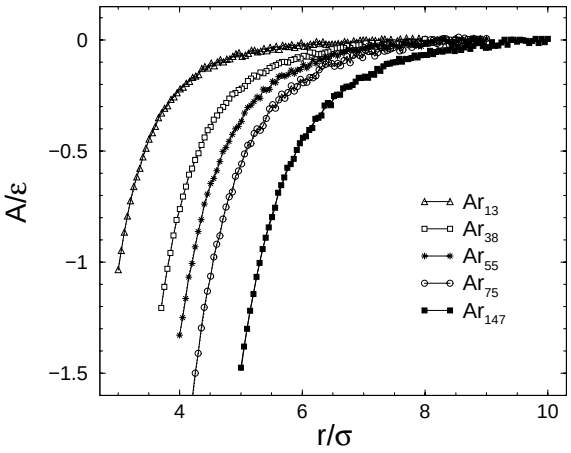

Fig. 2. Potential of mean force $A(r,T)$ at $T = 0.2\varepsilon/k_{\rm B}$ with the reference $A(\infty,T) = 0$. The dots are the results of MC simulations, the dashed lines are the fits on the form of equation (22).

problems can be found in references [19,20], as well as references inside. A possible generalization of these methods to rotating systems (including the conservation of angular momentum) has also been recently made [20].

Using also a constraint method, Weerasinghe and Amar investigated the effective potential energy between an argon atom and an argon cluster at finite temperature [21]. Due to the finite size of the cluster, they found that a pure attractive form C_6/r^6 was inappropriate to describe the interaction at long distances. Instead, they proposed another expression fitting well with the simulation, namely $C_6/(r-r_0)^6$. Except in the vicinity of r_0, this expression is pretty close to the result of the GV potential.

We performed a series of Metropolis Monte Carlo simulations on the systems Ar_N+Ar, for the set of sizes N = 13, 38, 55, 75 and 147, and for the four reduced LJ temperatures $T = 0.1$, 0.2, 0.3 and $0.4\varepsilon/k_{\rm B}$. The three "magic" sizes 13, 55 and 147 correspond to Mackay multilayer icosahedra, respectively with one, two and three layers. Ar_{38} has a truncated octahedral structure at $T = 0$, and Ar_{75} is decahedral [22]. Except for $N = 75$, all sizes investigated here are more or less spherical, while Ar_{75} is strongly oblate.

For each size and temperature, the range of r was about 10σ long, discretized into 100 bins δr of equal width. At fixed r, the MC simulation consisted of 10^5 cycles (1 cycle = $N+1$ individual steps) whose 2×10^4 first cycles were discarded for allowing thermalization.

We have plotted in Figure 2 the results of our simulations for the five clusters, at the temperature $T = 0.2\varepsilon/k_{\rm B}$. The fit of these curves on the form given by equation (22) is also given on this figure. In each case, we carried out a least-square minimization to find the parameters C_6, C_{12} and r_0 fitting best to the simulation points. It is worth noting that the fits are very good, leading to stable values of the three parameters when one changes the initial conditions in the numerical experiment. Such decent fits ensure the validity of the continuous model previously described.

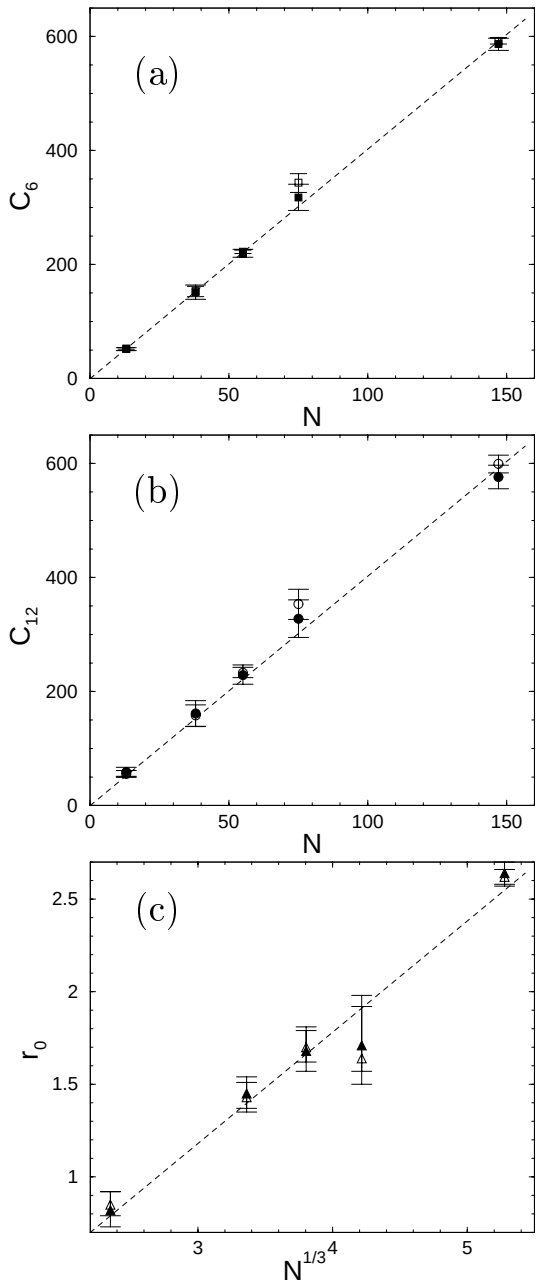

Fig. 3. (a) C_6 parameters fitted from the simulation results on the continuous model as a function of size N. The linear curve is simply $C_6(N) = 4N$. (b) Same results for the C_{12} parameters, with the linear curve $C_{12}(N) = 4N$. (c) Effective radius r_0 *versus* $N^{1/3}$ from the continuous model. The linear curve is $r_0(N) = 0.62[N^{1/3}-1]$. For all graphs, the results are shown for the two temperatures $T = 0.1\varepsilon/k_{\rm B}$ (empty squares) and $T = 0.4\varepsilon/k_{\rm B}$ (full squares).

In Figure 3 we have displayed the variation with N of the effective coefficients C_6 and C_{12} at finite temperature, as well as the variation with $N^{1/3}$ of the effective radius r_0 of the cluster. As can be seen from Figures 3a and 3b, both C_6 and C_{12} grow linearly with N in the whole range $13 \le N \le 147$. The growing rate is about 4.0 at the lowest temperature, and slightly decreases as T rises, especially above melting, for $T > 0.3\varepsilon/k_{\rm B}$.

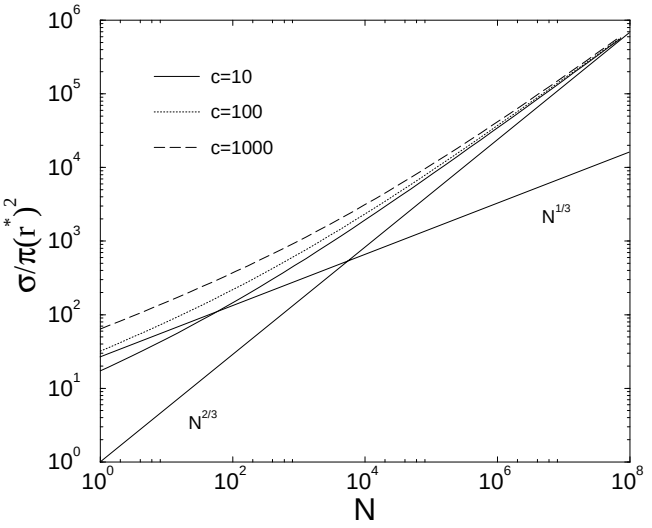

Fig. 4. Logarithmic plot of the sticking cross-section for the GV potential, as a function of the size N of the cluster, for three values of the adimensional parameter $c = C_{6\text{at.}}/K(r^*)^6$. Solid line: $c = 10$; dotted line: $c = 100$; dashed line: $c = 1000$. The limiting behaviours at small and large N are shown for $c = 100$.

This is not surprising, and similar temperature smoothing effects were observed in a previous thermodynamical study of the cluster-cluster interaction [19]. We see in Figure 3b that the error bars affecting the calculation for C_{12} are quite larger than those for C_6. This is in fact a simple consequence of the fact that the repulsive contribution is much smaller than the attractive one at such long distances. Figure 3c exhibits a linear behaviour of the radius r_0 *versus* $N^{1/3}$, apart from the value for $N = 75$ and $T \leq 0.3\varepsilon/k_\text{B}$. At this very special size, the cluster is strongly non spherical, and the effective radius is smaller than in a spherical configuration. When T is increased above $0.3\varepsilon/k_\text{B}$, the argon cluster melts and becomes more spherical; its effective radius increases. Excluding the data for $N = 75$, a linear fit of the variations of r_0 with $N^{1/3}$ approximately leads to $r_0 \approx 0.62\sigma[N^{1/3} - 0.98]$, which is in very good agreement with the GV model. Including the data corresponding to $N = 75$ gives a slightly different law as $r_0 \approx 0.59\sigma[N^{1/3} - 0.93]$, but still in agreement with the GV model.

Of course, extensive numerical calculations are difficult to achieve for clusters larger than 147 atoms. However, as the structure should become more and more spherical (first icosahedral, then FCC-bulklike), the linear behaviours of C_6 and C_{12} with N, of r_0 with $N^{1/3}$ have no reason to drop in the large cluster regime. Furthermore, as the size increases, the continuous model is less and less approximate. Hence the Gspann-Vollmar potential of equation (22) can be satisfactory chosen to represent the interaction between an argon atom and an argon cluster, even at finite temperature and for rather small sizes, provided that it is not used when the distance to the cluster is small enough to allow for isomerizations.

4 Theoretical cross-section

4.1 Calculation

Our calculation is based on the following method, which dates back to Langevin. If the centrifugal term $L^2/2\mu r^2$ (with μ the reduced mass) is added to the potential, the effective potential shows a centrifugal barrier of height $E_1(L)$ at a distance $r_1(L)$ depending on the angular momentum $L = \mu b v_\text{r}$, where b is the impact parameter. Once the atom overcomes this barrier, it may be considered to be stuck to the cluster, since the extra energy coming from the attractive part of the potential is very easily dissipated in the internal degrees of freedom of the cluster. To a given initial kinetic energy of the colliding system K, corresponds a maximum impact parameter b_0, given by $K = E_1(L)$ for $L^2 = 2\mu K b_0^2$. The sticking cross-section is then $\sigma = \pi b_0^2$. The relevant equations are the following:

$$2Kb_0^2 = r_1^3 V'(r_1); \tag{24}$$

$$K(r_1^2 - b_0^2) = r_1^2 V(r_1); \tag{25}$$

from which r_1 is to be eliminated. Let us begin with the long range part of the potential $V(r) = -C_6/r^6$, with $C_6 = NC_{6\text{at.}}$ proportional to N, the size of the cluster. We get $\sigma = 3\pi(C_6/4K)^{1/3}$, with a $N^{1/3}$ dependence for the cross-section. This first approximation breaks down when the cluster is big enough so that $b_0 - r_0$ becomes small compared to the cluster radius r_0. Of course, in this later case, the cross-section is close to the geometrical one and is given by $\sigma = \pi {r^*}^2 N^{2/3}$. The crossover size N_c is obtained when both cross-sections are equal, that is:

$$N_\text{c} = \frac{27C_{6\text{at.}}}{4{r^*}^6 K} = \frac{27}{4}c, \tag{26}$$

where we have introduced the non-dimensional parameter $c = C_{6\text{at.}}/{r^*}^6 K$.

In order to find the interpolation between the $N^{1/3}$ and $N^{2/3}$ behaviours, we study the case of the attractive part of the GV potential $V(r) = -C_6/(r^2 - r_0^2)^3$, still with C_6 proportional to N and $r_0 = N^{1/3} r^*$ proportional to $N^{1/3}$. We get

$$b_0^2 = \frac{3r_1^4 C_6}{K(r_1^2 - r_0^2)^4}; \tag{27}$$

$$b_0^2 = \frac{3r_1^4}{2r_1^2 + r_0^2}. \tag{28}$$

It is easy to eliminate b_0 to obtain the following equation:

$$\frac{C_6}{K}(2r_1^2 + r_0^2) = (r_1^2 - r_0^2)^4 \tag{29}$$

which can be numerically solved easily. The resulting cross-section as a function of N is plotted in Figure 4 for different values of the adimensional parameter c. Even for $c = 10$, the $N^{2/3}$ law is reached at a very high N value (10^4 or so). Actually, the mean exponent in the range $N = 1$–10^4 varies from 0.42 at $c = 1000$ to 0.52 at $c = 10$.

4.2 Results and crossover size for argon

Let us first discuss the expansion process in the case of argon. For an expansion starting near ordinary temperature and with moderate values of the source pressure p_0 (about 1 bar) and of the nozzle diameter d_0 (about 0.1 mm), it is well known that the final parallel temperature in the beam is of the order of 1 K, although the isentropic curve cuts the condensation domain near 60 K. This very low final temperature does not lead to condensation because the density in the beam is low. If now the source pressure is larger, condensation occurs and the final temperature of the clusters has been measured [3] to be 32 ± 2 K, a value corresponding to the solid-gas equilibrium near 10^{-6} mbar, estimated by extrapolating the saturation pressure equation of reference [23].

When condensation affects a large fraction of the expanding gas, after probably a brief phase of overcooling due to a delayed start of the condensation process, the temperature T_c should follow the condensation curve from about 60 K down to a final value close to 30 K and should not be constant as assumed in our simplified model. Knowing T_c, we can deduce the value of z_c^* from equation (9). It appears that the order of magnitude of z_c^* thus deduced is in the range of unity, whereas equation (9) is valid only for large z^*. However, any refinement of these questions is beyond the scope of the present paper and in any case, the fact that we want to compare our model to a simple scaling law makes these refinements useless at the present state of our understanding.

As soon as we know the value of the condensation temperature T_c, we can estimate the cross-section and the crossover size N_c which is the limit between the two regimes characterized by the value 1/3 and 2/3 of the exponent α. We use the value $C_{6at.} = 65$ au given by Dalgarno [24]. Taking for the mean value of the atom-cluster kinetic energy $K = k_B T_c$ with $T_c = 32 \pm 2$ K the temperature given by Farges *et al.* [3], we get $c \approx 160$, which leads to a crossover size $N_c \approx 1000$, and a mean scaling exponent $\alpha = 0.45$ over the size range 1–10^4, in very good agreement with the experimental results for α.

Let us re-express now our "theoretical" Γ parameter using the results of the previous paragraph. In the regime valid at low N values, the scaling exponent of the cross-section is $\alpha = 1/3$ and the relative atom-cluster kinetic energy is proportional to $k_B T_c$. Neglecting various constant multiplying factors, we get

$$\Gamma_{th} \propto p_0 d_0 C_{6at.}^{1/3} T_c^{11/12} / T_0^{9/4}. \quad (30)$$

If we compare the exponents of p_0, d_0 and T_0 in equation (1) giving Γ^* and in the present equation giving Γ_{th}, the comparison is very favorable, the only noticeable difference being on the exponent of d_0. The d_0 exponent is $q = 1$ in Γ_{th}, and $q = 0.85$ in Γ^*. The value $q = 1$ is expected [1,8,9,12] in the case of a cluster growth model based only on bimolecular processes, while $q = 0.5$ corresponds to the opposite limit of unimolecular reactions. The oversimplifier character of our model appears clearly here, but we think that our model is a sound first step in understanding the mean cluster size produced by condensation in supersonic expansion.

5 Conclusion

Let us recall the main results obtained in the present paper:

1. a simple model of condensation has been developed and in this model the final cluster size depends on the source parameters in a way very similar to the semi-empirical law introduced by Hagena;
2. from this model and experimental results concerning the mean size of the clusters, we have deduced the N-dependence of the sticking cross-section of an atom on a cluster of size N. This dependence is well represented by the equation $\sigma_N = \sigma_1 N^\alpha$ with α values slightly larger than 1/3;
3. a careful Monte Carlo study of the atom-cluster interaction potential has proven that the interaction potential introduced by Gspann and Vollmar is a very good approximation of the pair-wise additive Lennard-Jones potential, even at finite temperatures;
4. this analytic potential has been used to calculate the sticking cross-section in the Langevin approximation. The cross-section behaves like $N^{1/3}$ up to rather large N values and switches to the geometric scaling $N^{2/3}$ for very large N values. The cross-over between these two behaviours occurs near $N \approx 1000$ for argon. The very late onset of the geometrical scaling is an unexpected result which is surely important for the understanding of cluster growth in supersonic expansions and foreign atom pick-up by clusters [25] but also everywhere condensation is important. As such, this result can be interesting for modelling aerosol formation in many environments and this result will be important in very different fields: atmospheric physics, chemical engineering...

Finally, an interesting analogy with the laser can be done, as this is one of the best-known case of a dynamical phase transition. In the case of a single-mode laser, the interesting function is the probability distribution of the number n of photons in the mode: this function changes shape strongly from a quasi-thermal monotonously decreasing function when the laser is well below threshold to a function peaked near a large n value when the laser is over threshold. For the molecular beam, the function of interest is the distribution of cluster size N. For low source pressures, the beam contains a very small fraction of dimers and larger clusters and the distribution of cluster size is a rapidly decreasing function of the size N, as shown for instance by the experiments of Vasile and Stevie [26]. As soon as condensation starts, the distribution function changes shape, with a peak near a large N value and a peak for the monomer $N = 1$. Obviously the analogy is not complete and this is natural because the nonlinear equations describing the two problems are different.

We thank J.M. Mestdagh and M. Châtelet for communication of very helpful informations. We are indebted to Région Midi Pyrénées and MENRT for financial support of our laboratory.

References

1. O.F. Hagena, W. Obert, J. Chem. Phys. **56**, 1793 (1972).
2. J. Farges, B. Raoult, G. Torchet, J. Chem. Phys. **59**, 3454 (1973).
3. J. Farges, M.-F. de Feraudy, B. Raoult, G. Torchet, J. Chem. Phys. **84**, 3491 (1986).
4. A. Lallement, Ph.D. thesis, Orsay University, 1993.
5. U. Buck, R. Krohne, J. Chem. Phys. **105**, 5408 (1996).
6. M.Y. Benslimane, Ph.D. thesis, École Polytechnique, 1995.
7. A. De Martino, M. Benslimane, M. Châtelet, C. Crozes, F. Pradrère, H. Vach, Z. Phys. D **27**, 185 (1993).
8. O.F. Hagena, Z. Phys. D **4**, 291 (1987).
9. O.F. Hagena, G. Knop, R. Fromknecht, G. Linkes, J. Vac. Sci. Technol. A **12**, 282 (1994).
10. J. Gspann, H. Vollmar, in *Rarefied Gas Dynamics*, 8th Symposium, edited by K. Karamcheti (Academic Press, New York, 1974), p. 261.
11. J. Gspann, H. Vollmar, in *Rarefied Gas Dynamics*, 11th Symposium, edited by R. Campargue (CEA, Paris, 1979), Vol. II, p. 1193.
12. O.F. Hagena, Phys. Fluids **17**, 894 (1974).
13. C.E. Klots, Nature **327**, 222 (1987).
14. F. Calvo (unpublished results).
15. H. Ashkenas, F.S. Sherman, in *Rarefied Gas Dynamics*, 4th Symposium, edited by J.H. de Leeuw (Academic Press, New york, 1968), Vol. II, p. 84.
16. D.R. Miller, in *Atomic and Molecular Beam Methods*, edited by G. Scoles (Oxford University Press, New York, 1988), Vol. I, p. 14.
17. E. Fort, F. Pradère, A. De Martino, H. Vach, M. Châtelet, Eur. Phys. J. D **1**, 79 (1998).
18. T.L. Hill, J. Chem. Phys. **16**, 181 (1948).
19. F. Calvo, F. Spiegelmann, Phys. Rev. B **54**, 10949 (1996).
20. F. Calvo, Chem. Phys. Lett. **291**, 393 (1998).
21. S. Weerasinghe, F.G. Amar, J. Chem. Phys. **98**, 4967 (1993).
22. D.J. Wales, J.P.K. Doye, J. Phys. Chem. A **101**, 5111 (1997).
23. *Handbook of Chemistry and Physics*, edited by R.C. Weast, M.J. Astle, 63rd edn. (CRC Press, 1982-1983).
24. A. Dalgarno, Adv. Chem. Phys. **12**, 143 (1967).
25. J.M. Mestdagh, M.A. Gaveau, C. Gée, O. Sublemontier, J.P. Visticot, Int. Rev. Phys. Chem. **16**, 215 (1997).
26. M.J. Vasile, F.A. Stevie, J. Chem. Phys. **75**, 2399 (1981).